GSA Data Repository 2016326

Pu, J.P., Bowring, S.A., Ramezani, J., Myrow, P., Raub, T.D., Landing, E., Mills, A., Hodgin, E., and Macdonald, F.A., 2016. Dodging Snowballs: Geochronology of the Ediacaran Gaskiers Glaciation: Geology, v. 44, doi: 10.1130/G38284.1

U-Pb analytical procedures

Samples collected for geochronology from tuffaceous rocks generally range from 5 to 10 kg, and heavy mineral concentrates were separated from these by standard crushing, pulverization, magnetic and high-density liquid separation techniques. Hand selected zircons were pre-treated by a chemical abrasion (CA-TIMS) technique modified after Mattinson (2005) and spiked with the EARTHTIME ET535 mixed ^{205}Pb-^{233}U-^{235}U tracer (Condon et al., 2015; McLean et al., 2015) prior to dissolution and analysis, following the procedures described in Ramezani et al. (2011). Chemical abrasion consisted of annealing zircons in a furnace at 900°C for 60 hours, followed by leaching in 29 M HF at 210°C for 11.5 to 13 hours. Pre-treatment of this intensity caused extensive disintegration or near-complete dissolution of some zircons, but was deemed necessary in order to mitigate the effects of Pb loss due to accumulated radiation damage in zircons of Precambrian age.

Measurement of Pb and U isotopic ratios were carried out on either the VG Sector 54 or the Isotopx X62 multi-collector, thermal-ionization mass spectrometers equipped with Daly (photomultiplier) ion-counting systems at the MIT Isotope Lab. Data reduction including tracer deconvolution, date calculation, and propagation of uncertainties was carried out using computer applications Tripoli and U-Pb Redux (Bowring et al., 2011; McLean et al., 2011). A total of 59 single zircons were analyzed from eight tuffaceous samples bracketing the glacial diamictites and strata preserving Ediacaran fossils. Complete U-Pb isotopic data appear in Table DR1.

Sample dates are calculated based on the weighted mean ^{206}Pb/^{238}U date of a statistically coherent cluster of the youngest zircon analyses from each sample after excluding older analyses interpreted as xenocrystic or detrital, and are reported at 95% confidence level. In two cases (samples GCI-neg7.75 and OBJP-01), younger analyses interpreted to have been affected by persistent Pb loss were excluded from weighted mean calculations. Sample dates that are mutually distinct outside 2σ internal uncertainty and obey stratigraphic order are considered meaningful approximations of the depositional age. Calculated sample dates and detailed uncertainties are listed in Table 1 and illustrated in date distribution plots of Figs. 2 and 3 and concordia plots of Fig. DR3.

In the past, it was customary to derive zircon ages from weighted mean ^{207}Pb/^{206}Pb dates (or concordia intercepts) for rocks of Precambrian age because of the precision provided by the abundance of ^{207}Pb in old samples, as well as the general insensitivity of ^{207}Pb/^{206}Pb dates to Pb loss. With enhanced control on Pb loss made possible by the chemical abrasion technique, ^{206}Pb/^{238}U dates now offer greater advantages over the corresponding ^{207}Pb/^{206}Pb measurements in terms of accuracy. In addition, it has been demonstrated that in statistically equivalent sets of high-precision U-Pb analyses, the

$^{207}Pb/^{206}Pb$ dates are systematically older than the $^{206}Pb/^{238}U$ dates by up to several percent, possibly because of inaccuracies in the mean values of one or both of the U decay constants (e.g., Schoene et al., 2006). This systematic age discordance that may amount to ~0.5% in samples of Gaskiers age has rendered the $^{207}Pb/^{206}Pb$ dates (and concordia intercept dates) essentially obsolete in modern U-Pb zircon geochronologic studies.

Sample Description and U-Pb Geochronology

St. Mary's Bay – Trepassey Bay, southern Avalon Peninsula

In the central Avalon Peninsula of Newfoundland, diverse Neoproterozoic volcanic, pyroclastic, and volcaniclastic rocks of the Harbour Main Group are intruded by granitoids of the Holyrood Intrusive Suite, and both are unconformably overlain by predominantly deep-water siliciclastic deposits of the upper Neoproterozoic Conception Group (e.g. Williams and King, 1979). In the area of this study, the basal Conception Group consists of graded beds of volcaniclastic sandstone, siliciclastic mudstone, and chert of the Mall Bay Formation with an exposed thickness of ~ 800 m (base of the formation is not exposed). These strata are interpreted to have been deposited in a deep-water environment, well below storm-wave base (Myrow, 1995). Discrete, thin beds of limestone are present locally in this formation as well. The Mall Bay Formation is overlain by the Gaskiers Formation, a lithologically distinct, weakly bedded diamictite with only minor stratified siliciclastic strata and agglomerate and a maximum thickness of 250 to 300 m. The outcrop distribution of the Gaskiers Formation outlines conjugate anticlines and synclines. The lower contact with the Mall Bay Formation appears sharp but conformable. Although dropstones are present in the upper Mall Bay Formation at other localities (Fig. DR1B), we did not observe dropstones in the Mall Bay Formation at Great Colinet Island. Thus, the contact between the Mall Bay and Gaskiers formation may be regionally diachronous. Poorly sorted, angular polymictic and striated clasts and dropstones set in a sandy matrix characterize the diamictites of the Gaskiers Formation (Fig. DR1A), and have been interpreted to represent marine deposition from floating ice (e.g. Brückner and Anderson, 1971; Carto and Eyles, 2011; Eyles and Eyles, 1989; Gravenor, 1980; Williams and King, 1979). At some localities, the Gaskiers diamictite is capped by a thin carbonate bed (Fig. DR1D). The overlying Drook Formation with a thickness of ~ 1500 m is the thickest and most widely distributed unit of the Conception Group throughout the Avalon Peninsula. Its extensive siliciclastic mudstone, siltstone, and sandstone interbedded with chert and tuff (Fig. DR1E) conformably overlie the Gaskiers Formation. The overlying Briscal Formation is a coarse sandy facies above the Drook Formation (Williams and King, 1979). The ~ 400 m thick, thin- to medium-bedded sandstone and shale of the Mistaken Point Formation overlie and interfinger with the Briscal and Drook formations, and are exposed mostly along coastal sections. The Mistaken Point Formation is known for its abundant Ediacaran fossil forms that are preserved on distinct bedding planes beneath thin (1 cm or less) tuff horizons. It grades upward into the Trepassey Formation of the St. John's Group.

Sample GCI-neg7.75 – This sample was collected from an 8 cm thick aquagene ash bed from the upper Mall Bay Formation at the southwestern end of Great Colinet Island (Fig. DR1C). The conformable contact between the Mall Bay Formation and the diamictites of the overlying Gaskiers Formation is exposed at this locality within the southeast-dipping strata along the coastal cliffs. The ash bed occurs 7.75 m below the Gaskiers contact. Eight out of 11 single zircon grains analyzed from this sample form a statistically coherent cluster with a weighted mean $^{206}Pb/^{238}U$ date of 580.34 ± 0.52/0.62/0.88 Ma and a MSWD of 0.36. One slightly older analysis (z1) at 582.9 Ma suspected of being xenocrystic and two younger analyses (z3, z5) at 574.2 Ma and 577.0 Ma interpreted to have persistent Pb loss have been excluded from the date calculation. The above weighted mean date represents the best estimate for the age of volcanic eruption and deposition of ash in the upper Mall Bay Formation. The alternative interpretation of the youngest analysis representing the depositional age would be entirely inconsistent with the stratigraphy (see below).

Sample GCI-neg6.55 – This sample is from a ca. 45 cm thick aquagene ash bed from the upper Mall Bay Formation and was collected from the same locality as GCI-neg7.75, only 1.2 m higher in the section, i.e., closer to the basal Gaskiers contact. All 9 single zircon analyses from this sample form a tight cluster with a weighted mean $^{206}Pb/^{238}U$ date of 580.90 ± 0.40/0.53/0.82 Ma and a MSWD of 1.1. Both U-Pb dates from the upper Mall Bay Formation at the Great Colinet Island overlap within 2σ internal uncertainty, while sample GCI-neg6.55 provides a more robust date and a more reliable maximum estimate for the age of the Gaskiers diamictite.

Sample NoP-0.9 – An ash bed was collected from the basal Drook Formation at North Point, north of the town of St. Mary's across St. Mary's Harbour. The southeast-dipping strata of the Drook Formation at this locality form the eastern flank of a north-northeast-plunging anticline with the Mall Bay and Gaskiers formations exposed at its core. The sample is from 0.9 m above the upper Gaskiers contact. A coherent cluster of 5 zircon analyses from this sample yielded a weighted mean $^{206}Pb/^{238}U$ date of 579.88 ± 0.44/0.52/0.81 Ma (MSWD = 0.82), which serves as the best estimate for the age of the basal Drook Formation.

Sample Drook-2 – A 28 cm thick, light green, yellow weathering, highly cleaved ash bed was sampled from the upper part of the Drook Formation at Pigeon Cove (eastern Trepassey Bay), 3.5 km south of the village of Portugal Cove South and 0.75 km northwest of the old hamlet of Drook (Stop 1B of Landing et al., 1988). The large bedding surface exposed as the result of erosion of the overlying ash layer displays numerous large Ediacaran fossils including characteristic 'pizza disc' Ivesheadiomorph specimens. The stratigraphic ranges of many Ediacaran taxa abundant in the overlying Mistaken Point Formation start at this bedding surface (Liu et al., 2012). A good estimate for the age of this key stratigraphic level is provided by a weighted mean $^{206}Pb/^{238}U$ date of 570.94 ± 0.38/0.46/0.77 Ma (MSWD = 0.33), based on 5 overlapping zircon analyses from the Drook-2 ash.

Sample MPMP-33.56 – Collected from a 0.5 cm thick, dark-colored tuff intercalated with deep-water turbiditic mudstone and tuffaceous siltstone of the upper part of the type section of the Mistaken Point Formation (33.56 m above the base of the exposed section) that crops out at Mistaken Point, 7.5 km southwest of Cape Race (Figure 11B of Landing et al., 1988). Ivesheadiomorph and spindle-shaped Ediacaran fossils are exposed on the prominent bedding plane. All five analyzed zircons from this sample form a tight cluster with a weighted mean $^{206}Pb/^{238}U$ date of 566.25 ± 0.35/0.48/0.77 Ma (MSWD = 1.3), which constrains the age of the upper Mistaken Point Formation.

Old Bonaventure, Bonavista Peninsula

On the Bonavista Peninsula, geochronology samples were taken near Old Bonaventure from a 163.0 m thick measured section of the Rocky Harbour Formation (Fig. DR2A). The base of the section consists of 41.2 m of coarse white to gray, bidirectionally cross-bedded sandstone and granule- to pebble-clast conglomerate with thin laminated interbeds of purple siltstone. Volcanic clasts with feldspar phenocrysts are the most common lithology in the conglomerates and in the sandstone units, where they occur as outsized clasts. The thin (1 - 3 cm) purple siltstone interbeds are most common at the base of 5 - 10 m thick coarsening upwards parasequences. Above these strata is a 3.2 m thick unit of volcanic tuffs and interbedded siltstone, which is overlain by 8.9 m of sandstone coarsening up into pebble conglomerate with up to 5 cm thick interbeds of purple siltstone. These units are most similar to Monk Bay, Kings Cove Lighthouse, and Cape Bonavista facies (Normore, 2011; O'Brien and King, 2002). The 19.7 m thick massive diamictite of the Trinity facies sharply overlies the underlying sediments. It has a purple-colored matrix and contains a range of sand- to cobble-sized clasts dominated by volcanics that have feldspar phenocrysts, similar to descriptions of rocks of the Bull Arm Formation. A 0.5 m thick transitional sandstone unit separates the massive diamictite from overlying dropstone-bearing stratified diamictite. The 16 m thick stratified diamictite consists of mm- to cm-scale graded beds of sandstone and siltstone that are punctured by bed-penetrating dropstones (Fig. DR1F). The dropstones are associated with wispy lenses of coarse sandstone and are interpreted to represent ice-rafted debris. Clasts generally decrease in size and frequency up-section, but larger clasts reappear in the upper 1-2 m of stratified diamictite. Above the stratified diamictite is another 2.7 m of massive diamictite characterized by a white sandstone matrix with purple siltstone interbeds and very few clasts. In total, the Trinity diamictite is ~39 m thick and is overlain by 44.8 m of gray-green to blue-green, finely laminated siltstone with rare sandstone lenses. These fine-grained sediments, which are similar to Normore's (2011) descriptions of the Kings Cove North facies of the upper Rocky Harbour Formation, are succeeded by a suite of volcanic tuffs, agglomerates, and flows. The tuffs are distinct peach-colored, silicified beds that are up to 2-3 cm thick and interbedded with blue siltstone for about 3.3 m. Above the interbedded tuffs and siltstone is a 13.7 m thick basaltic bed that contains pink lithic clasts. This is succeeded by at least another 9 m of significantly reworked volcaniclastic rocks and mafic flows containing reworked rounded mafic clasts.

The 52.2 m section measured in Cat Cove is fault-bounded and well-exposed on the shoreline (Fig. DR2B). In the basal 3.8 m of exposure below the Trinity diamictite, a

series of pebble conglomerates fine upwards into coarse-grained sandstone and gritty laminated siltstone. The basal 2.9 m of glacigenic deposits consist of sandy matrix massive diamictite with up to boulder-sized clasts, stratified diamictite with up to 3 cm lonestones, and interbedded pebble conglomerate and siltstone with convolute lamination. A massive diamictite with a dark green gritty mudstone matrix continues for 21.2 m with a single interbed of lonestone-bearing stratified diamictite at 12.5–13.1 m. In the overlying stratified diamictite, which continues for 16.8 m, laminated siltstone and mm-scale sandstone lenses are punctured by bed-penetrating dropstones that decrease in size and frequency up-section. Sparse gravel to cobble-sized rounded clasts occur in the uppermost stratified diamictite. The diamictite is overlain by 0.2 m of medium- to coarse-grained sandstone and transitions up-section into 4 m of fine-grained planar to wavy-laminated pistachio-colored, siliceous siltstone. Symmetric, large amplitude wave ripples are present 5–10 m above the top of the diamictite that are interpreted to represent storm-generated wave ripples that formed below fair-weather wave-base. Well-preserved flame structures and convolute bedforms occur on a storm wave ripple surface ~10 m above the top of the diamictite near the top of the section.

The Trinity Pond section (Fig. DR2C) was measured along NL-230. Beneath the first appearance of diamictite is ~ 60 m of cross-stratified, coarse-grained sandstone with minor pebble-clast conglomerate and laminated purple siltstone. Tidal wave ripples displaying interference patterns are well-exposed on a dipslope 32.8 m below the diamictite. The basal ~7 m of the Trinity facies consists of unsorted clast-supported diamictite that transitions gradually into massive, matrix-supported diamictite. The overlying stratified diamictite consists of mm- to cm-scale graded beds of sandstone and siltstone that are punctured by bed-penetrating dropstones, which decrease in size and frequency up-section. The dropstones are associated with wispy lenses of coarse sandstone and are interpreted to represent ice-rafted debris. The uppermost 1-2 m of stratified diamictite contains sparse pebble to cobble-sized clasts. The overlying pistachio-colored, siliceous siltstone contains wavy laminations and thin interbeds of coarse-grained sandstone and granule-clast conglomerate. Dewatering structures occur on a storm wave ripple surface ~ 6 m above the top of the stratified diamictite.

Sample B1552 42.2 – A tuff was collected 42.2 m above the base of the Old Bonaventure section, 11.1 m below the base of the diamictite, from a massive, light-yellow bed with pink horizons, and is interpreted as an air-fall ash. In thin section, the tuff has a cryptocrystalline texture with quartz phenocrysts. Six high-precision zircon analyses from this sample gave a weighted mean $^{206}Pb/^{238}U$ date of 579.63 ± 0.15/0.29/0.68 Ma (MSWD = 0.018), which best represents the age of eruption and deposition of the tuff.

Sample OBJP-03 – This sample of purple diamictite was collected from 60.0 m above the base of the Old Bonaventure section, 6.7 m above the base of the Trinity diamictite facies. With the exception of two older analyses with $^{206}Pb/^{238}U$ dates of 631.56 ± 0.50 Ma and 612.39 ± 0.63 Ma interpreted as detrital zircon, the remaining four analyses overlap within uncertainty with a weighted mean $^{206}Pb/^{238}U$ date of 579.35 ± 0.33/0.42/0.75 Ma (MSWD = 0.73). The latter provides a maximum estimate for the age of diamictite deposition.

Sample OBJP-01 – This sample was collected from a silicified, peach-colored, tuff bed interstratified with blue-green, silicified siltstones at 140.0 m above the base of the section (Fig. DR1G) and 47.8 m above the top of the Trinity diamictite in this section (Fig. DR2A). Twelve zircon analyses from this sample display a complex array of dates, ranging from 580.58 ± 0.90 Ma to 571.02 ± 0.48 Ma. The majority (nine) of the analyses form a statistically coherent cluster with a weighted mean $^{206}Pb/^{238}U$ date of 579.24 ± 0.17/0.30/0.69 Ma (MSWD = 1.3), which can be interpreted as the best age estimate for the deposition of the tuff, invoking persistent Pb loss for two distinctly younger zircons (z2 and z11) that do not overlap in error.

References

Bowring, J. F., McLean, N. M., and Bowring, S. A., 2011, Engineering cyber infrastructure for U–Pb geochronology: Tripoli and U–Pb Redux: Geochemistry Geophysics Geosystems, v. 12, p. Q0AA19.

Brückner, W. D., and Anderson, M. M., 1971, Late Precambrian glacial deposits in southeastern Newfoundland, a preliminary note: Proceedings of the Geological Association of Canada, v. 24, p. 95-102.

Carto, S. L., and Eyles, N., 2011, The deep-marine glaciogenic Gaskiers Formation, Newfoundland, Canada: Geological Society, London, Memoirs, v. 36, no. 1, p. 467-473.

Condon, D., Schoene, B., McLean, N., Bowring, S., and Parrish, R., 2015, Metrology and traceability of U–Pb isotope dilution geochronology (EARTHTIME Tracer Calibration Part I): Geochimica et Cosmochimica Acta, v. 164, p. 464-480.

Eyles, N., and Eyles, C. H., 1989, Glacially□influenced deep□marine sedimentation of the Late Precambrian Gaskiers Formation, Newfoundland, Canada: Sedimentology, v. 36, no. 4, p. 601-620.

Gravenor, C., 1980, Heavy minerals and sedimentological studies on the glaciogenic Late Precambrian Gaskiers Formation of Newfoundland: Canadian Journal of Earth Sciences, v. 17, no. 10, p. 1331-1341.

Hiess, J., Condon, D. J., McLean, N., and Noble, S. R., 2012, $^{238}U/^{235}U$ Systematics in Terrestrial Uranium-Bearing Minerals: Science, v. 335, no. 6076, p. 1610-1614.

Jaffey, A. H., Flynn, K. F., Glendenin, L. E., Bentley, W. C., and Essling, A. M., 1971, Precision measurements of half-lives and specific activities of 235U and 238U: Physical Review C, v. 4, p. 1889-1906.

Landing, E., Narbonne, G. M., Myrow, P., Benus, A. P., and Anderson, M. M., 1988, Faunas and depositional environments of the Upper Precambrian through Lower Cambrian, southeastern Newfoundland: New York State Museum Bulletin, v. 463, no. 1, p. 8-52.

Liu, A. G., McIlroy, D., Matthews, J. J., and Brasier, M. D., 2012, A new assemblage of juvenile Ediacaran fronds from the Drook Formation, Newfoundland: Journal of the Geological Society, v. 169, no. 4, p. 395-403.

Mattinson, J. M., 2005, Zircon U-Pb chemical abrasion ("CA-TIMS") method: combined annealing and multi-step partial dissolution analysis for improved precision and accuracy of zircon ages: Chemical Geology, v. 220, p. 47-66.

McLean, N., Bowring, J., and Bowring, S., 2011, An algorithm for U□Pb isotope dilution data reduction and uncertainty propagation: Geochemistry, Geophysics, Geosystems, v. 12, no. 6.

McLean, N. M., Condon, D. J., Schoene, B., and Bowring, S. A., 2015, Evaluating uncertainties in the calibration of isotopic reference materials and multi-element isotopic tracers (EARTHTIME Tracer Calibration Part II): Geochimica et Cosmochimica Acta, v. 164, p. 481-501.

Myrow, P. M., 1995, Neoproterozoic rocks of the Newfoundland Avalon zone: Precambrian Research, v. 73, no. 1, p. 123-136.

Normore, L. S., 2011, Preliminary findings on the geology of the Trinity map area (NTS 2C/06), Newfoundland: Current Research (2011), Newfoundland and Labrador Department of Natural Resources, v. Geological Survey, Report 11-1, p. 273-293.

O'Brien, S., and King, A., 2002, Neoproterozoic stratigraphy of the Bonavista Peninsula: preliminary results, regional correlations and implications for sediment-hosted stratiform copper exploration in the Newfoundland Avalon Zone: Current research (2002). Newfoundland Department of Mines and Energy, Geological Survey, Report, p. 02-01.

Ramezani, J., Hoke, G. D., Fastovsky, D. E., Bowring, S. A., Therrien, F., Dworkin, S. I., Atchley, S. C., and Nordt, L. C., 2011, High-precision U-Pb zircon geochronology of the Late Triassic Chinle Formation, Petrified Forest National Park (Arizona, USA): Temporal constraints on the early evolution of dinosaurs: Geological Society of America Bulletin, v. 123, no. 11-12, p. 2142-2159.

Schoene, B., Crowley, J. L., Condon, D. J., Schmitz, M. D., and Bowring, S. A., 2006, Reassessing the uranium decay constants for geochronology using ID-TIMS U–Pb data: Geochimica et Cosmochimica Acta, v. 70, no. 2, p. 426-445.

Williams, H., and King, A. F., 1979, Trepassey map area, Newfoundland, Geological Survey of Canada, v. 389-391.

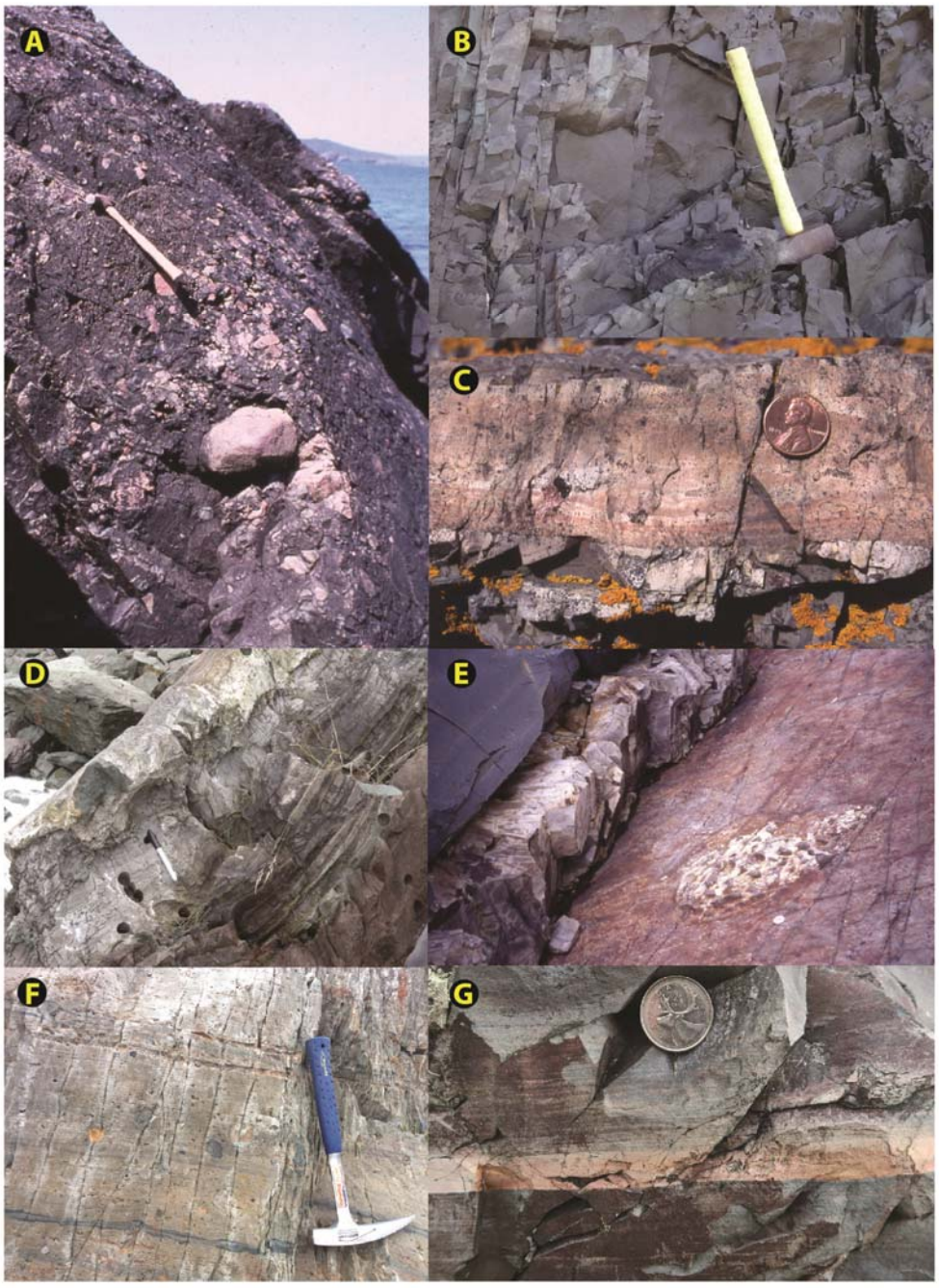

Figure DR1. A) Basal Gaskiers Formation exposed on the southwestern shore of the Great Colinet Island, St. Mary's Bay, hammer for scale. B) Black-colored basaltic dropstone in the upper Mall Bay Formation south of Harbour Main, hammer for scale. C) Ash GCI-neg7.75 sampled on the southeastern shore of Great Colinet Island, St. Mary's Bay, and dated at 580.34 ± 0.52 Ma, U.S. penny for scale. D) Basal Drook cap carbonate at Harbour Main, Sharpie and 1-inch diameter paleomagnetic drill holes for scale. E) Ediacaran Ivesheadiomorph fossil exposed on the bedding surface underneath a tuff bed in the Drook Formation at Portugal Cove South, near sample Drook-2 dated at 570.94 ± 0.38 Ma. F) Laminated Trinity diamictite with dropstones at New Bonaventure, hammer for scale. G) Ash OB-JP-01 dated at 579.24 ± 0.17 Ma, Canadian quarter for scale.

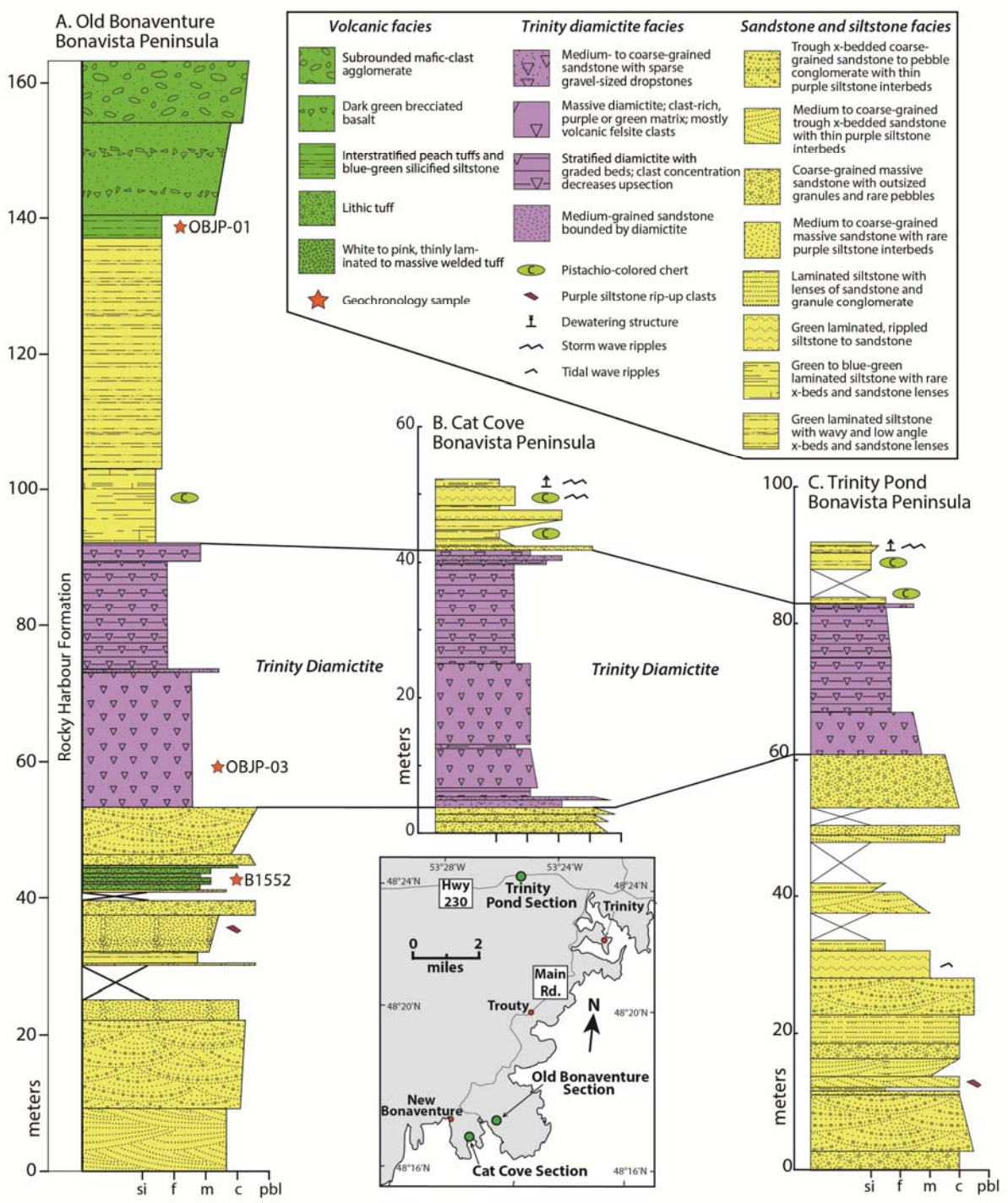

Figure DR2. Stratigraphic sections of the Rocky Harbour Formation at Bonavista Peninsula from A) Old Bonaventure, B) Cat Cove, and C) Trinity Pond. Inset shows the locations of the measured sections.

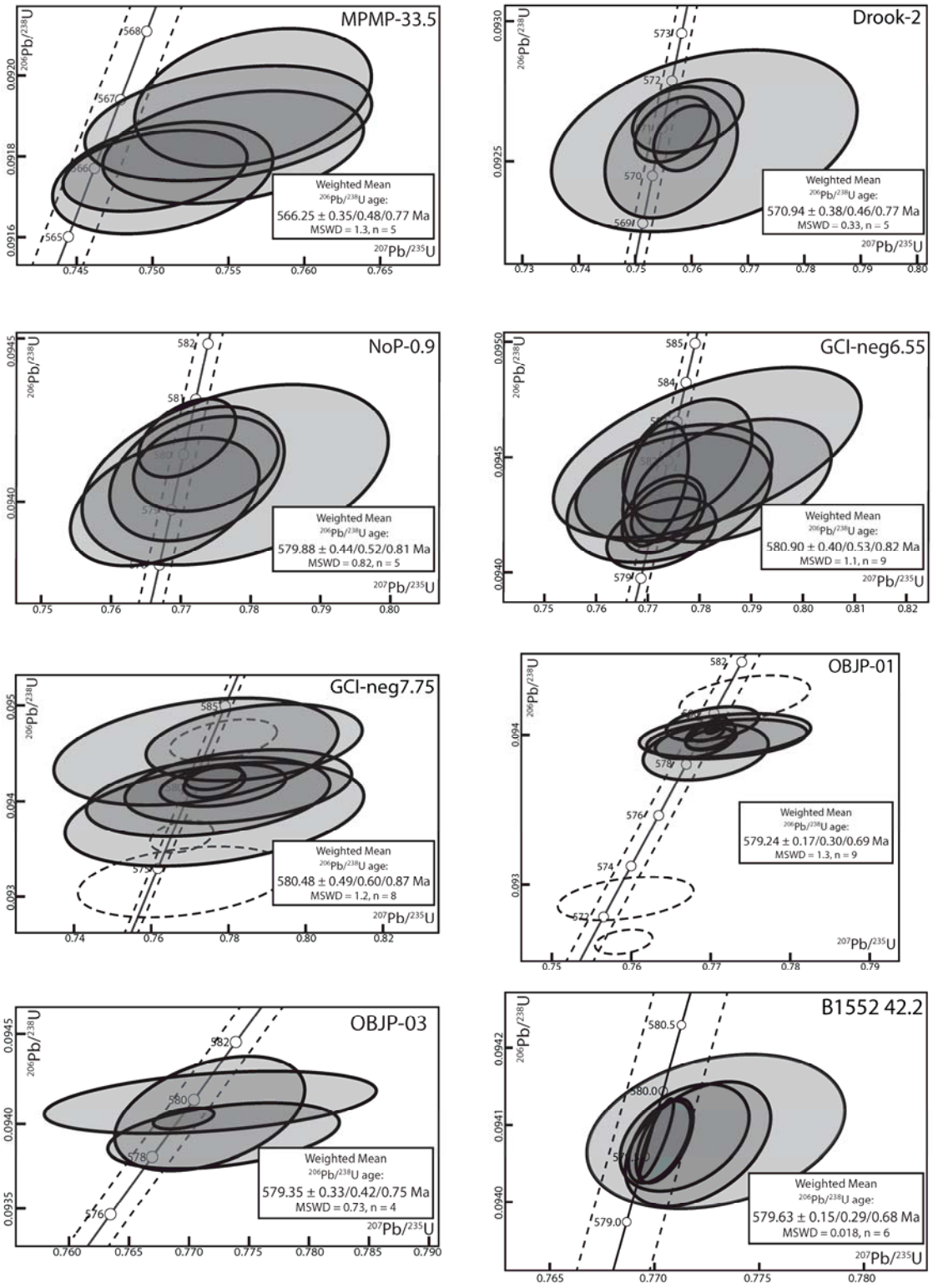

Figure DR3. Concordia plots for the analyzed zircons from the tuffaceous samples of this study. Dashed lines delineate the concordia error envelope. Analyses excluded from date calculation are shown with open ellipses. See Table DR1 for complete U-Pb data and Table 1 for details of calculated dates and reported uncertainties.

TABLE DR1

U-Pb data for analyzed zircon from Late Neoproterozoic tuffaceous rocks of eastern Newfoundland.

	Composition					Ratios						Ages (Ma)				
Sample	Pb_c[‡]	Pb*[‡]	Th	^{206}Pb[§]	^{208}Pb[#]	^{206}Pb[††]	err	^{207}Pb[††]	err	^{207}Pb[††]	err	^{206}Pb	err	^{207}Pb	err	corr.
Fractions[†]	(pg)	Pb_c	U	^{204}Pb	^{206}Pb	^{238}U	(2σ%)	^{235}U	(2σ%)	^{206}Pb	(2σ%)	^{238}U	(2σ)	^{206}Pb	(2σ)	coef.
MPMP-33.56: *Mistaken Point Formation, Mistaken Point, Southeastern Avalon Peninsula (46°37'32.46"N, 53° 9'45.88"W)*[¶]																
z2	0.2	16.9	0.47	1027.0	0.147	0.091945	(.19)	0.75662	(1.03)	0.05971	(.99)	**567.0**	**1.0**	592	21	0.30
z5	0.2	13.8	0.49	837.4	0.152	0.091882	(.15)	0.75499	(1.25)	0.05962	(1.21)	**566.66**	**0.84**	589	26	0.33
z3	0.2	15.5	0.52	929.0	0.162	0.091822	(.15)	0.75531	(1.14)	0.05969	(1.10)	**566.31**	**0.82**	591	24	0.31
z1	0.2	21.8	0.52	1303.9	0.161	0.091764	(.11)	0.75016	(.81)	0.05932	(.78)	**565.96**	**0.59**	578	17	0.34
z4	0.2	19.1	0.64	1106.3	0.200	0.091747	(.15)	0.75067	(.97)	0.05937	(.93)	**565.86**	**0.82**	580	20	0.33
z2	0.2	16.9	0.47	1027.0	0.147	0.091945	(.19)	0.75662	(1.03)	0.05971	(.99)	**567.0**	**1.0**	592	21	0.30
Drook-2: *Drook Formation, Pigeon Cove, Southeastern Avalon Peninsula (46°41'6.94"N, 53°15'38.03"W)*[¶]																
z4	1.2	16.5	1.37	813.9	0.425	0.092661	(.14)	0.75930	(1.29)	0.05946	(1.24)	**571.26**	**0.77**	583	27	0.36
z1	0.3	28.6	1.66	1322.3	0.516	0.092613	(.13)	0.75660	(.88)	0.05928	(.84)	**570.97**	**0.69**	576	18	0.40
z2	0.5	33.3	1.67	1531.4	0.519	0.092583	(.13)	0.75904	(.76)	0.05949	(.73)	**570.79**	**0.68**	584	16	0.30
z3	2.5	5.9	1.41	300.4	0.438	0.092573	(.35)	0.76226	(3.55)	0.05975	(3.45)	**570.7**	**1.9**	593	75	0.33
z5	0.5	14.4	1.27	727.6	0.393	0.092532	(.25)	0.75638	(1.55)	0.05931	(1.50)	**570.5**	**1.4**	578	33	0.29
NoP-0.9: *Drook Formation, North Point, St. Mary's Bay, Southeastern Avalon Peninsula (46°56'17.87"N, 53°34'30.39"W)*[¶]																
z1	0.4	25.2	1.03	1328.3	0.319	0.094195	(.13)	0.77090	(.90)	0.05938	(.85)	**580.30**	**0.71**	580	19	0.45
z2	0.5	12.5	0.94	684.0	0.292	0.094086	(.22)	0.77232	(1.62)	0.05956	(1.56)	**579.7**	**1.2**	587	34	0.33
z3	0.4	12.5	0.95	679.2	0.294	0.093999	(.21)	0.76770	(1.76)	0.05926	(1.68)	**579.1**	**1.2**	576	37	0.41
z4	0.8	7.2	1.19	381.6	0.371	0.094082	(.29)	0.77778	(2.82)	0.05999	(2.72)	**579.6**	**1.6**	602	59	0.38
z5	0.5	16.8	1.19	860.1	0.371	0.094115	(.15)	0.77360	(1.34)	0.05964	(1.30)	**579.83**	**0.85**	590	28	0.29
GCl-neg6.55: *Mall Bay Formation, Great Colinet Island, St. Mary's Bay, Southeastern Avalon Peninsula (46°57'33.14"N, 53°43'7.82"W)*[¶]																

z5	0.1	20.3	1.54	962.7	0.479	0.094520	(.39)	0.78150	(3.81)	0.05999	(3.61)	**582.2**	**2.2**	602	78	0.55
z3	0.2	16.0	1.49	769.8	0.463	0.094489	(.28)	0.77768	(1.60)	0.05972	(1.51)	**582.0**	**1.6**	592	33	0.40
z2	0.4	9.5	1.65	450.2	0.514	0.094399	(.28)	0.78640	(2.43)	0.06045	(2.33)	**581.5**	**1.6**	619	50	0.38
z1	0.4	9.0	1.39	449.4	0.433	0.094390	(.27)	0.77506	(2.45)	0.05958	(2.36)	**581.4**	**1.5**	587	51	0.38
z4	0.2	48.6	1.66	2232.2	0.516	0.094384	(.28)	0.77153	(.82)	0.05931	(.75)	**581.4**	**1.6**	578	16	0.42
z8	0.3	8.9	1.63	427.2	0.506	0.094324	(.30)	0.77411	(2.55)	0.05955	(2.46)	**581.1**	**1.6**	586	53	0.34
z7	0.2	33.4	1.60	1558.5	0.497	0.094264	(.14)	0.77346	(.86)	0.05954	(.81)	**580.71**	**0.77**	586	18	0.40
z6	0.2	25.0	1.44	1207.3	0.447	0.094253	(.18)	0.77305	(1.04)	0.05951	(.98)	**580.64**	**0.99**	585	21	0.38
z9	0.4	17.8	1.73	817.1	0.536	0.094169	(.16)	0.77263	(1.37)	0.05953	(1.31)	**580.15**	**0.91**	586	28	0.38
GCl-neg7.75: ***Mall Bay Formation, Great Colinet Island, St. Mary's Bay, Southeastern Avalon Peninsula (46°57'32.69"N, 53°43'8.79"W)***[¶]																
z1	0.4	12.2	1.27	618.8	0.394	0.094638	(.23)	0.77869	(1.78)	0.05970	(1.70)	582.9	1.3	592	37	0.41
z10	0.6	5.7	1.26	301.9	0.391	0.094615	(.42)	0.78665	(3.56)	0.06033	(3.45)	**582.8**	**2.3**	614	74	0.32
z11	0.5	4.2	0.98	238.0	0.305	0.094518	(.59)	0.77159	(4.77)	0.05923	(4.60)	**582.2**	**3.3**	575	100	0.34
z9	0.3	21.5	1.12	1113.2	0.349	0.094251	(.14)	0.77622	(.95)	0.05976	(.91)	**580.63**	**0.76**	594	20	0.33
z8	0.2	18.8	0.83	1044.4	0.257	0.094199	(.17)	0.77636	(1.02)	0.05980	(.98)	**580.32**	**0.94**	595	21	0.32
z7	0.6	9.5	1.18	498.2	0.366	0.094167	(.23)	0.77855	(2.09)	0.05999	(2.02)	**580.1**	**1.3**	602	44	0.32
z6	0.8	5.2	1.09	284.9	0.340	0.094157	(.40)	0.78255	(3.75)	0.06030	(3.64)	**580.1**	**2.2**	614	79	0.33
z4	0.9	4.8	0.98	269.6	0.304	0.094047	(.44)	0.77474	(4.07)	0.05977	(3.95)	**579.4**	**2.4**	594	86	0.33
z12	0.9	4.2	1.16	229.7	0.362	0.093864	(.58)	0.77638	(4.98)	0.06002	(4.81)	**578.4**	**3.2**	603	104	0.35
z5	0.6	19.7	1.11	1025.0	0.345	0.093632	(.18)	0.76790	(1.07)	0.05951	(1.02)	577.0	1.0	585	22	0.31
z3	0.6	5.3	0.86	303.5	0.266	0.093156	(.40)	0.76839	(3.56)	0.05985	(3.45)	574.2	2.2	597	75	0.33
OBJP-01: ***Rocky Harbour Formation, Old Bonaventure, Bonavista Peninsula (48°17'2.57"N, 53°24'58.26"W)***																
z8	0.2	19.8	0.95	1067.0	0.296	0.094242	(.16)	0.77427	(1.06)	0.05961	(1.01)	580.58	0.90	589	22	0.40

z7	0.3	27.5	1.02	1454.7	0.316	0.094074	(.12)	0.77021	(.76)	0.05941	(.72)	**579.59**	**0.67**	581	16	0.39
z9	0.2	156.3	0.80	8602.6	0.249	0.094066	(.06)	0.77065	(.17)	0.05945	(.14)	**579.54**	**0.31**	582.5	3.2	0.61
z1	0.2	85.5	1.02	4479.7	0.316	0.094015	(.06)	0.76961	(.27)	0.05940	(.24)	**579.24**	**0.34**	580.7	5.3	0.47
z3	0.3	51.9	0.93	2780.7	0.289	0.093999	(.10)	0.76995	(.41)	0.05943	(.37)	**579.15**	**0.55**	582.0	8.1	0.44
z4	0.6	14.4	1.14	748.7	0.353	0.093997	(.15)	0.77180	(1.40)	0.05958	(1.35)	**579.13**	**0.85**	587	29	0.34
z5	2.1	13.6	0.67	787.5	0.209	0.093972	(.14)	0.77203	(1.31)	0.05961	(1.27)	**578.99**	**0.77**	589	27	0.33
z6	0.3	55.4	1.17	2813.9	0.363	0.093971	(.08)	0.77006	(.41)	0.05946	(.39)	**578.98**	**0.43**	583.0	8.4	0.41
z10	0.2	33.9	1.10	1755.7	0.341	0.093950	(.11)	0.76797	(.65)	0.05931	(.61)	**578.86**	**0.63**	578	13	0.39
z12	0.2	19.6	0.71	1118.2	0.221	0.093886	(.20)	0.76937	(1.02)	0.05946	(.99)	**578.5**	**1.1**	583	21	0.28
z11	0.2	19.1	1.13	987.8	0.352	0.092908	(.15)	0.75930	(1.12)	0.05930	(1.08)	572.71	0.84	577	23	0.37
z2	0.2	50.8	1.13	2602.4	0.353	0.092620	(.09)	0.75905	(.48)	0.05946	(.46)	571.02	0.48	583.2	9.9	0.31
OBJP-03: ***Trinity Diamictite, Rocky Harbour Formation, Old Bonaventure, Bonavista Peninsula (48°17'3.84"N, 53°25'4.08"W)***																
z2	0.4	35.6	0.75	1991.4	0.234	0.102931	(.08)	0.86361	(.53)	0.06088	(.51)	631.56	0.50	634	11	0.36
z1	0.2	30.0	0.64	1733.4	0.198	0.099656	(.11)	0.82812	(.64)	0.06030	(.61)	612.39	0.63	613	13	0.35
z5	0.6	11.0	0.84	614.5	0.262	0.094127	(.20)	0.77178	(1.79)	0.05949	(1.73)	**579.9**	**1.1**	584	38	0.38
z4	0.2	23.4	0.95	1256.5	0.295	0.094062	(.36)	0.77173	(1.03)	0.05953	(.94)	**579.5**	**2.0**	586	20	0.41
z3	0.2	65.7	0.79	3635.3	0.246	0.094033	(.07)	0.76955	(.33)	0.05938	(.30)	**579.34**	**0.37**	580.1	6.6	0.45
z6	0.3	17.6	0.82	981.2	0.254	0.093931	(.21)	0.77288	(1.25)	0.05970	(1.18)	**578.7**	**1.1**	592	26	0.40
B1552-42.2: ***Rocky Harbour Formation, Old Bonaventure, Bonavista Peninsula (48°17'3.34"N, 53°25'5.16"W)***																
z4	0.3	23.8	0.72	1350.7	0.223	0.094092	(.11)	0.77293	(.80)	0.05961	(.77)	**579.69**	**0.59**	588	17	0.27
z6	0.3	51.1	0.79	2828.8	0.247	0.094084	(.07)	0.77144	(.40)	0.05949	(.38)	**579.64**	**0.41**	584.3	8.2	0.38
z1	0.2	584.5	1.08	30107.2	0.335	0.094083	(.05)	0.77010	(.10)	0.05939	(.06)	**579.64**	**0.30**	580.5	1.4	0.84
z2	0.3	151.8	0.82	8307.9	0.256	0.094080	(.06)	0.77049	(.18)	0.05942	(.15)	**579.62**	**0.32**	581.7	3.3	0.55
z3	0.2	133.3	0.95	7081.0	0.296	0.094078	(.06)	0.77024	(.19)	0.05941	(.17)	**579.61**	**0.31**	581.0	3.7	0.53

z5	0.3	45.0	0.84	2464.6	0.262	0.094075	(.09)	0.77208	(.45)	0.05955	(.42)	**579.59**	**0.48**	586.3	9.1	0.42

Notes: Corr. coef. = correlation coefficient. Age calculations are based on the decay constants of Jaffey et al. (1971).

† All analyses are single zircon grains and pre-treated by the thermal annealing and acid leaching (CA-TIMS) technique. Data used in age calculations are in bold.

‡ Pb_c is total common Pb in analysis. Pb* is radiogenic Pb concentration.

§ Measured ratio corrected for spike and fractionation only.

Radiogenic Pb ratio.

†† Corrected for fractionation, spike, blank, and initial Th/U disequilibrium in magma. Mass fractionation corrections of 0.25%/amu and 0.18%/amu ± 0.04%/amu (atomic mass unit) was applied to single-detector Daly analyses on Sector54 and X62 instruments, respectively, unless Pb double-spike was used. All common Pb is assumed to be blank. Total procedural blank was less than 0.1pg for U. $^{238}U/^{235}U = 137.818 \pm 0.022$ (2σ) after Hiess et al. (2012). Blank isotopic composition: $^{206}Pb/^{204}Pb = 18.15 \pm 0.47$, $^{207}Pb/^{204}Pb = 15.30 \pm 0.29$ and $^{208}Pb/^{204}Pb = 37.11 \pm 0.87$.

¶ Coordinates are accurate to within 100 meters.